

Optical microring resonator filter design trade-offs

Alastair D. McAulay, Michael R. Corcoran, Christopher J. Florio, and Ian B. Murray
Lehigh University, ECE Department, Bethlehem, PA, USA.

ABSTRACT

A microring resonator, a circular waveguide adjacent to a straight waveguide, performs selective band-stop filtering for optical telecommunications. Small size and versatility of functionality allow many microrings to be incorporated into a single integrated optic circuit. We desire small size, less than 20 μm radius; low insertion loss in band-stop outside resonance; perfect cancellation to zero in band-stop at resonance; and low refractive index difference between core and cladding. These requirements are conflicting: conventional silicon waveguides cannot achieve low enough loss at the desired bend radius. Current approaches use different materials with higher refractive index differences. Analysis and simulation provide evaluation of the trade-offs. Further, we propose, for the first time, conventional waveguides using Bragg reflectors surrounding the microring to reduce loss for improved performance. Simulation shows feasibility of this approach.

Keywords: Integrated optics, planar integrated optics, resonators, microring resonators, Bragg microring resonators, microstructure devices, integrated optic filters

1. INTRODUCTION

Microring waveguide resonators have been analyzed for use as integrated optic filters^{10,15} and applied to a range of functionality² and applications.^{7,12,14} Microring resonators are candidates for combining into high-density complex integrated optic systems on a chip⁶—in a similar manner to VLSI in electronics—because of their small size and flexibility for performing different functions. The range of functions is expanded by incorporating nonlinear and gain material.

However, small rings, less than 20 μm , require tight bends which typically incur large losses. A large difference in refractive index between core and cladding will reduce loss but fabrication becomes more expensive. A range of different materials have been used in experiments that allow large index differences: III-V materials,⁴ Silicon Nitride, (SiN)^{5,11} silicon oxynitride (SiON),⁹ silicon on insulator (SOI),³ and Germanium doped silica.¹ An integrated circuit device incorporating ring resonators is available commercially⁸ that uses a proprietary glass based material with index difference up to 10%. In this paper we provide analysis and simulation for performing trade-offs and we explore, for the first time, Bragg reflection waveguiding to reduce loss. Lower loss permits smaller rings for higher density circuits or smaller refractive index differences to make fabrication and interconnection to fiber less expensive.

Previously, a specific microring structure with Bragg reflection guiding was analyzed,¹³ but coupling this microring structure to a straight waveguide appears difficult if not impossible. We use a different structure: a conventional waveguide microring between Bragg reflective rings. In our case, coupling between the straight waveguide and the microring is not affected significantly by the presence of the Bragg reflectors.

2. SINGLE MICRORING RESONATOR

Figure 1 shows a commonly arising configuration involving a straight waveguide, a ring and a directional coupler that couples the waveguide and ring. The ring and waveguide are spaced apart to control the coupling coefficient κ and hence s and t . The circuit can act as a bandstop filter. A small part s of the light entering at a_1 is coupled to the microring at b_2 , the rest (most of the input) t passes to the output at b_1 . When the input is not at the resonant frequency, this is the output at b_1 . However, at resonant frequency, the part coupled into the ring builds up to a high value in the ring so that it is large enough (and out of phase) to cancel the input and reduce the output at b_1 to zero.

Further author information: E-mail: adm5@lehigh.edu, Telephone: 1 610 758 6079, www.eecs.lehigh.edu/~amcaulay.
Active and Passive Optical Components for WDM Communications IV Conference, SPIE 5595-48, Oct. 2004

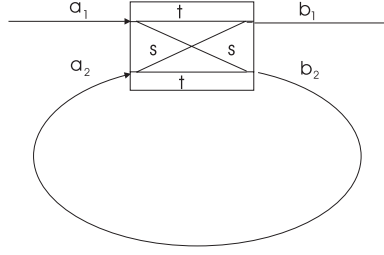


Figure 1. Optical waveguide coupled to a micro-ring

2.1. Design criteria and trade-offs

2.1.1. Criteria for waveguide design

For a rectangular waveguide, at a specified wavelength, we select width between first order and second order mode cut-offs; this allows propagation of only a single fundamental (lowest frequency) mode. A range of permissible widths meet this criteria. If width is selected close to the fundamental mode cut-off, the field extends far from the waveguide. This reduces losses in a straight waveguide by reducing effects of wall roughness, but increases losses in a ring because the extremities of the tails extending into the cladding can no longer keep up with the bend; this results in leaky waves that dissipate outwards from the curved waveguide. If the width is selected too close to the second order mode cut-off, or for very large refractive index differences, the field is tightly confined in the core. Then, coupling distances between straight and ring waveguides becomes very small which requires high lithographic resolution; alternatively, other coupling arrangements are necessary.

2.1.2. Criteria for resonance

Resonance occurs when light traveling through a complete loop of the ring has the same phase as it had at the start of the loop. Therefore, each loop reinforces previous loops and energy builds up in the ring resonator. This can be written,

$$\beta L = 2m\pi \quad (1)$$

where β is phase or propagation constant (radians/m) in ring, L is length of ring (m), and m an arbitrary integer. As $\beta = 2\pi n_e/\lambda$, with n_e the equivalent refractive index of the waveguide, we can write the length L of the circumference as an integer number of wavelengths,

$$L = \frac{m\lambda}{n_e} \quad (2)$$

Unfortunately n_e is difficult to compute because it depends on the percentage of light traveling in the core (the higher refractive index) versus that in the cladding (the lower refractive index). This in turn depends on the difference in refractive index between core and cladding and the closeness to fundamental mode cut-off, as explained previously.

2.1.3. Criteria for cancellation of field in bandstop filter operation

The coupling length l and coupling coefficient κ (adjusted by altering separation between straight waveguide and ring) are selected to provide 90° phase shift on crossing from one side of the coupler to the other. In figure 1, light passing from a_1 to b_2 and then from a_2 to b_1 , crosses the coupler twice, developing a 180° phase shift to become out of phase with that reaching b_1 from the straight waveguide a_1 . The two fields will therefore cancel each other by destructive interference. However, for a quality bandstop filter, at resonance, in addition to being 180° out of phase, the two fields must have the same intensity to provide complete cancellation. The fields are the same intensity if, in the steady state, the power entering the ring at b_2 through the coupling s equals the power lost in traveling once around the ring. Power that is not coupled into the ring arrives at the exit at the top right, figure 1, therefore, the loss around the ring equals the loss passing through the upper side of the directional coupler, from a_1 to b_1 .

Next we derive the equations that verify the intuitive criteria discussed previously for complete cancellation at resonance. The steady state input-output equations for the circuit of figure (1) are^{15,10}

$$\begin{bmatrix} b_1 \\ b_2 \end{bmatrix} = (1 - \gamma)^{0.5} \begin{bmatrix} t & s \\ s & t \end{bmatrix} \begin{bmatrix} a_1 \\ a_2 \end{bmatrix} \quad (3)$$

where $t = \cos(\kappa l)$, $s = -j\sin(\kappa l)$, κ is coupling coefficient, l is coupling length, γ is intensity insertion loss coefficient. For intensity attenuation coefficient in the ring ρ , the amplitude coefficient is $\rho/2$ (from $\exp\{-\rho L/2\}^2 = \exp\{-\rho L\}$), and the output of the ring is

$$a_2 = b_2 \exp\left(-\frac{\rho L}{2} - j\beta L\right). \quad (4)$$

Defining

$$x = (1 - \gamma)^{0.5} \exp\left(-\frac{\rho L}{2}\right) \quad (5)$$

we can write the intensity transmittance of the optical ring resonator in a form similar to that for the well known Fabry-Perot resonator.

$$T = \left|\frac{b_1}{a_1}\right|^2 = (1 - \gamma) \left[1 - \frac{(1 - x^2)(1 - t^2)}{(1 - tx)^2 + 4tx\sin^2(\beta L/2)}\right] \quad (6)$$

From equation (6), the maximum and minimum transmission occurs when the last term in the denominator of equation (6), $4tx\sin^2(\beta L/2)$ is maximum or zero respectively,

$$T_{max} = (1 - \gamma) \frac{(x + t)^2}{(1 + xt)^2} \quad (7)$$

$$T_{min} = (1 - \gamma) \frac{(x - t)^2}{(1 - xt)^2} \quad (8)$$

The output cancels to zero for a band stop filter at resonance when $T_{min} = 0$ or from equation (8) and (5),

$$t = x \quad \text{or} \quad t = (1 - \gamma)^{0.5} \exp\left(-\frac{\rho L}{2}\right) \quad (9)$$

This specifies that the transmission loss t from a_1 to b_1 must equal the loss in traveling once around the ring times a factor for transmission insertion loss.

Other useful characteristics of the microring resonator are full width at half maximum

$$\delta(\beta l) = \frac{2(1 - xt)}{\sqrt{xt}} \quad (10)$$

and finesse, indicative of the number of channels possible,

$$F = \frac{2\pi}{\delta(\beta l)} = \frac{\pi\sqrt{xt}}{(1 - xt)} \quad (11)$$

2.2. Single microring simulation results

Figure 2 shows the layout for a single embedded microring of radius $18.5 \mu\text{m}$, width $1.033 \mu\text{m}$, refractive indices 1.5 for the core and 1 for the cladding, separation between microring and straight waveguide of $0.23 \mu\text{m}$, operating at wavelength $1.55 \mu\text{m}$.

From simulation, figure 3, shows that at resonance, the amplitude in the ring is brighter than that in the input at the top left because of constructive interference of light in successive loops in the ring. Further, the output of the straight waveguide at the top right is reduced as appropriate for a bandstop filter at resonance.

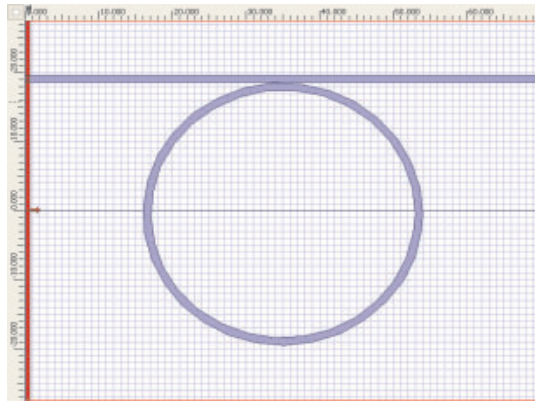


Figure 2. Layout for single microring

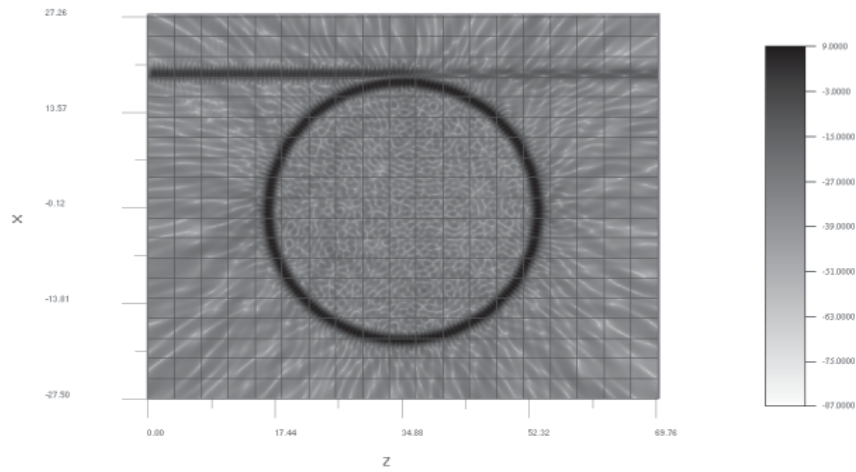


Figure 3. Amplitude from simulation for single microring

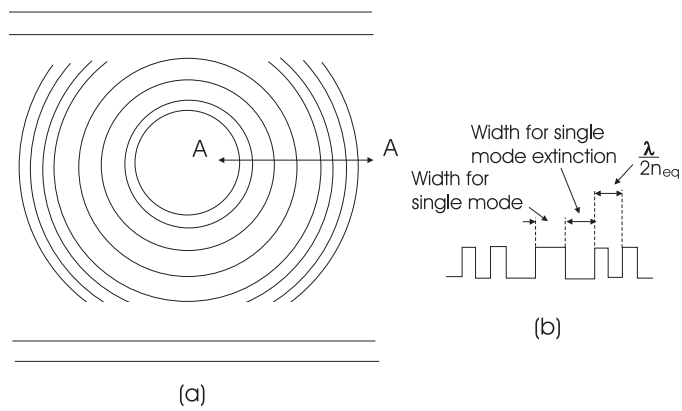


Figure 4. Layout for illustrating principle for Bragg microring simulation: (a) Plan view, (b) Cross section

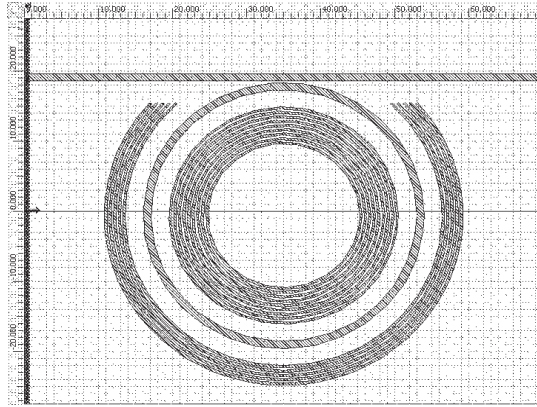


Figure 5. Layout for Bragg microring simulation

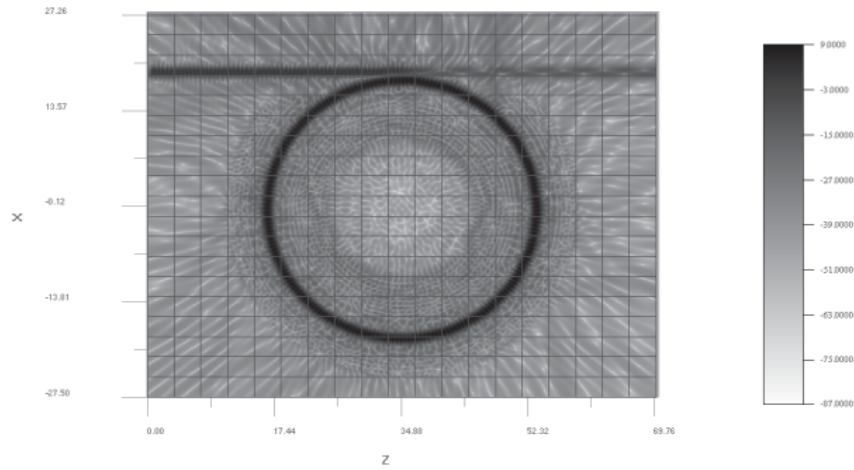


Figure 6. Amplitude from simulation for Bragg reflected microring

3. DESIGN OF BRAGG REFLECTOR MICRORING RESONATOR

3.1. Design criteria for microring resonator with Bragg reflector guiding

Figure 4(a) shows the principle for the Bragg reflected microring and 4(b) a typical cross section. The single microring system of figure 2 is modified to reduce losses from the microring bend by the addition of Bragg reflecting waveguides. The period of the Bragg reflectors is $\lambda/(2n_{eq})$ as shown, where n_{eq} is the equivalent refractive index for one Bragg period. The waveguide is then too narrow to propagate any modes along it at the frequency of interest. The outside rings reflect back power escaping as leaky waves due to the waveguide bend, inside rings reflect back energy that passes through the microring waveguide. The outside rings are cut off in the vicinity of the straight waveguide to prevent coupling directly into them.

Bragg reflecting waveguides to reduce loss have been analyzed¹³ for a case with a low refractive index center surrounded by reflecting Bragg ring waveguides. However, our structure differs by having a waveguide of high refractive index in the center so that a directional coupler can couple in and out of the ring from a straight waveguide. Reduction of loss allows smaller rings or reduction of refractive index difference between cladding and core.

3.2. Simulation results for microring with Bragg reflector guiding

Figure 5 shows the layout used for simulation of the ring with Bragg reflectors. The core microring and waveguide are identical to those in figure 2. In addition there are five Bragg reflecting rings on the outside of the microring resonator and eight rings on the inside. Figure 6 shows the resulting optical amplitude from a simulation with the layout of figure 5. Comparison of figure 6 with figure 3 shows that the Bragg rings suppress leaky waves and consequently bend losses relative to the single microring case.

4. CONCLUSION

Microring resonators provide potential for high density optical integrated circuits because of great versatility and small size. Criteria for designing microring resonators were identified and equations derived. An improved microring resonator was proposed, for the first time, in which Bragg reflecting rings reduce loss. Simulation showed that the loss is reduced by the presence of the Bragg reflecting rings. Reducing loss improves performance by allowing smaller rings or reducing index difference between core and cladding for less expensive fabrication and interconnection to fiber.

ACKNOWLEDGMENTS

OptiFDTD from Optiwave Systems Inc. was used for simulations.

REFERENCES

1. Bourdon, G, Alibert, G.; Beguin, A.; Bellman, B.; Guiot, E. "Ultralow loss ring resonators using 3.5% index-contrast Ge-doped silica waveguides," *IEEE Photonics Technology Letters*, **15**(5), pp. 709-11, 2003.
2. Choi, J.M., Lee, R.K., and Yariv, A., "Control of critical coupling in a ring resonator-fiber configuration: application to wavelength-selective switching, modulation, amplification, and oscillation," *Optics Letters*, **26**(16), pp. 1236-1238, 2001.
3. Dumon, P., Bogaerts, W., Wiaux, V., Wouters, J., Beckx, S., Van Campenhout, J., Taillaert, D., Luysaert, B., Bienstman, P., Van Thourhout, D., Baets, R. "Low-loss SOI photonic wires and ring resonators fabricated with deep UV lithography," *IEEE Photonics Technology Letters*, **16**(5), pp. 1328-30, 2004.
4. Grover, R, Absil, P.P.; Van, V.; Hryniewicz, J.V.; Little, B.E.; King, O.; Calhoun, L.C.; Johnson, F.G.; Ho, P. T. "Vertically coupled GaInAsP-InP microring resonators," *Optics letters*, **26**(8), pp. 506-8, 2001.
5. Haeiwa, H., Naganawa, T., and Kokubun, Y, "Wide range center wavelength trimming of vertically coupled microring resonator filter by direct UV irradiation to SiN ring core," *IEEE Photonics Technology Letters*, **16**(1), pp. 135-7, 2004.
6. Little, B, Chu, S.T.; Pan, W.; Kokubun, Y., "Microring resonator arrays for VLSI photonics," *IEEE Photonics Technology Letters*, **12**(3), pp. 323-5, 2000.
7. Little, B. E., Chu, S. T., Haus, H. A., Foresi, I, and Lain, J. P, "Microring resonator channel dropping filter," *J. Lightwave Technology*, **15**(6), 1997.
8. Little Optics Inc., see Littleoptics.com
9. Melloni, A, Costa, R.; Monguzzi, P.; Martinelli, M. "Ring-resonator filters in silicon oxynitride technology for dense wavelength-division multiplexing systems," *Optics Letters*, **28**(17), pp. 1567-9, 2003.
10. K. Okamoto, *Fundamentals of Optical Waveguides*, Academic Press, San Diego, 2000.
11. Philipp, H. T., Svendsen, W.; Andersen, K.N.; Hubner, J.; Povlsen, J.H. "Measurement of optical nonlinearity in silicon rich nitride waveguide ring resonators," *Electronics letters*, **39**(16), pp. 1184-5, 2003.
12. Poon, J, Scheuer, J.; Yariv, A, "Wavelength-selective reflector based on a circular array of coupled microring resonators," *IEEE Photonics Technology Letters*, **16**(5), pp. 1331-3, 2004.
13. Scheuer, J.; Yariv, A., "Two-dimensional optical ring resonators based on radial Bragg resonance," *Optics Letters*, **28**(17), pp. 1528-1530, 2003.
14. Suzuki, S, Hatakeyama, Y.; Kokubun, Y.; Sai Tak Chu, "Precise control of wavelength channel spacing of microring resonator add-drop filter array," *Journal of lightwave technology*, **20**(4), pp. 745-50, 2002.
15. Yariv, A., "Universal relations for coupling of optical power between microresonators and dielectric waveguides," *Electronics Letters*, **36**(4), pp. 321-322, 2000.